NJC

Preparation of novel magnetic and fluorescent CS-Fe3O4@CdSeS nanoparticles for simultaneous removal and optical determination of trace copper ion

Journal:	*New Journal of Chemistry*
Manuscript ID:	NJ-ART-07-2014-001235.R1
Article Type:	Paper
Date Submitted by the Author:	24-Sep-2014

Complete List of Authors:	Xiao, Ling; Wuhan University, School of Resource and Environmental Science Xie, Chengli; Wuhan University, School of Resource and Environmental Science Peng, Shanzhi; Wuhan University, School of Resource and Environmental Science Shi, Xiaowen; Wuhan University, School of Resource and Environmental Science

Preparation of novel magnetic and fluorescent CS-Fe_3O_4@CdSeS nanoparticles for simultaneous removal and optical determination of trace copper ion

Chengli Xie, Ling Xiao*, Shanzhi Peng and Xiaowen Shi

School of Resource and Environmental Science, Hubei Biomass-Resource Chemistry and Environmental Biotechnology Key Laboratory, Wuhan University, Wuhan 430072, P R China

*Corresponding author: Fax: +862768763162 Tel: +862768778652 E-mail: xiaoling9119@whu.edu.cn

Postal address: The Luojia Mountain of Wuchang, Wuhan City, Hubei Province, P R China (430072)

Abstract: Novel magnetic and fluorescent CS-Fe_3O_4@CdSeS nanoparticles (MF-CSNPs) were synthesized by incorporating Fe_3O_4-chitosan nanoparticles and mercaptopropionic acid capped alloyed CdSeS quantum dots into a chitosan matrix via electrostatic interaction. The structure and properties of these novel MF-CSNPs were characterized by UV-visible, FL, XRD, ICP-AES, VSM and TEM. MF-CSNPs are found to adsorb copper ion with high saturation adsorption capacity of 260 mg g^{-1}, above 95.0%wt of copper ion can be enriched and removed from aqueous systems in minutes by manipulating MF-CSNPs with an external magnetic field. The fluorescence signals of MF-CSNPs could be quenched effectively by adsorbed copper ions. Linear relationships are established between the relative fluorescence intensity of MF-CSNPs and the concentration of copper ion. The linear range and limit of detection for copper ion depend on the concentration of MF-CSNPs. The linear range varies in the concentration range 0.21-80 $\mu g \cdot L^{-1}$ or 0.40-700 $\mu g \cdot L^{-1}$, with the lowest limit of detection 0.022 $\mu g \cdot L^{-1}$ calculated after enrichment. Trace copper ions in water can be simultaneously removed and determined with MF-CSNPs.

Keywords: magnetic fluorescent nanoparticles/ chitosan/ determination/ removal/ copper ion

1. Introduction

Copper as one of the essential trace nutrients for life, its deficiency would cause many diseases such as anemia, neutropenia, and bone abnormalities. Nevertheless, it possesses potential toxicity if load exceeds tolerance.[1] Inappropriate compartmentalization or elevation of copper ion in human body can cause neurodegenerative disorders and cause damage to the liver and kidneys.[2,3] In recent years, copper is predominantly being used in agriculture and various engineering purposes such as electrical, electroplating, energy, petrochemical industries, which results in increasing accumulation of copper ion in the environment. Copper ions can enter into human body via accumulating in the food chain. Therefore, it is necessary to determine and remove copper ions from contaminated aqueous environment.

Different techniques are used for determination of copper ion. In particular, the fluorescent optical probes attract increasing attention due to their high sensitivity and simplicity of manipulation. Quantum dots (QDs) are promising fluorescent probes because of their unique properties such as narrow luminescent and broad absorption spectra.[4,5] In recent years, various QDs fluorescent probes have been explored for detection of copper ion.[6] The excellent QDs probes with high fluorescence quantum yields (QYs) are the guarantees of high sensitivity detection to metal ions. Researches about QDs with excellent fluorescence properties have been carried out, *e. g.* core-shell quantum dots,[7-9] surface functionalized quantum dots,[10,11] doping semiconductor nanocrystals,[12-14] and alloyed quantum dots.[15,16] Han and his co-workers enhanced the QYs of CdSe from ~1% to ~9.9% by increasing the preparation temperature from 100 ℃ to 180 ℃.[7] Afterward, zhang *et al*. in 2014 enhanced the QYs of CdSe from ~9.9% to 10.9% by treating 3-MPA capped CdSe QDs with imidazole and decreased the detection limit for copper ion.[10]

In addition, a number of studies have been performed on adsorption materials for removal of copper ion in aqueous solutions.[17] Recently, increasing attention is paid to incorporate magnetic nanoparticles with quantum dots to obtain bifunctional materials with both magnetism and optical properties, which can be applied in broad fields including drug targeting, biosensors, chemosensor, magnetic resonance imaging and diagnostic.[18-21] The bifunctional materials for simultaneous removal and optical determination of copper ion have been reported. Wang and his co-workers successfully developed Fe_3O_4@C@CdTe for detection of copper ion in 2011.[22] Yang *et al.* in 2013 reported a glutathione-modified magnetic fluorescent Fe_3O_4@ZnS for simultaneous detection and removal of copper ion.[23] Chitosan is the N-deacetylated derivative of chitin. It is recommended as suitable functional material for removal of copper ion due to their biocompatibility, non-toxicity, biodegradability, and good ability in complexing with copper ion.[24,25] Magnetic chitosan nanoparticles exhibit good adsorption behaviour toward copper ion and are easy to be recovered with magnetic field.[26] Liu *et al*. prepared magnetic and fluorescent

bifunctional chitosan nanoparticles (MF-CSNPs) for optical determination of copper ion.[27]

Alloyed CdSeS QDs with a CdSe-rich core and a CdS-thick shell exhibit higher quantum yield (QY≈23.9%) than bare CdSe (QY≈10.9%).[10,16] In this paper, the novel magnetic and fluorescent bifunctional chitosan nanoparticales (MF-CSNPs) were prepared by encapsulating water soluble Fe_3O_4-chitosan magnetic nanoparticles and mercaptopropionic acid capped alloyed CdSeS QDs into chitosan matrix via electrostatic interaction. The obtained MF-CSNPs were applied to simultaneous removal and optical detection of copper ions in aqueous solution.

2. Materials and methods

2.1 Materials

Cadmium chloride, sodium hydroxide, acetic acid, isopropanol, anhydrous sodium sulfite, ferric chloride hexahydrate and ferrous chloride tetrahydrate were purchased from Sinopharm Chemical Reagent Co., Ltd (Shanghai, china, http://sinoreagent.con.alibaba.com/). Selenium powder was purchased from Tianjin Chemical Reagent Research Institute (Tianjin, China, http://tjshxsjy.cn.china.cn/). Disodium hydrogen phosphate was purchased from Tianjin Bo Di Chemical Co., Ltd (Tianjin, China, http://bodi000.cn.chemnet.com/). Monopotassium phosphate was purchased from Tianjin North Glass Co., Ltd (Tianjin, China, http://bfhbcaoyang.b2b.hc360.com/). Ammonium hydroxide was purchased from Kaifeng Dong Da chemical Co., Ltd (Kaifeng, China, http://pingmeidongda.suliao.biz/). Mercaptopropionic acid was purchased from Aladdin Reagent Co., Ltd (Shanghai, China, http://www.aladdin-e.com/). Chitosan was purchased from Zhejiang Golden-shell Biochemical Co., Ltd (Zhejiang, China, http://www.jinkechitin.com/). All chemicals were used without purification. All solutions were prepared with doubly distilled water.

2.2 Characterization

Ultraviolent-visible spectra and fluorescence emission spectra were recorded on a UV-1601 spectrophotometer and Hitachi F-4500 fluorescence spectrophotometer, respectively. Nanocrystal size and morphology were characterized by using a JEOL JEM-2010 FEF electron microscope operated at an acceleration voltage of 120 kV (Tokyo, Japan). X-ray diffraction (XRD) patterns were recorded on a X' Pert Pro X-ray diffractometer with Cu Kα irradiation (λ = 1.5406 Å) (PANalytical, Netherlands). The room temperature magnetization was performed by JDAW-2000B vibrating sample magnetometer in the -20000 to 20000 Oe magnetic field range (Changchun, China). Zeta potentials of the samples were measured by Malvern Zetasizer Nano ZS (Malvern, England). The elementary analysis was carried out with IRIS Intrepid II XSP ICP-atomic emission spectroscopy (Massachusetts, American). Flame atomic adsorption spectrometry was obtained from a TAS-990 (Beijing, China). Graphite furnace atomic adsorption spectrometry was obtained from a PerkinElmer AAnalyst 800 (Massachusetts, American).

2.3 Synthesis of Fe_3O_4-chitosan magnetic nanoparticles

The synthesis of Fe_3O_4-chitosan magnetic nanoparticles was carried out according to the reported procedure.[28] 200 mL 0.20% (v/v) HAc aqueous solution of 2.0 g L^{-1} chitosan was added in 500 mL 3-neck round-bottom flask. Then 44 mL aqueous solution containing 0.70 g $FeCl_3 6H_2O$ and 0.30 g $FeCl_2 4H_2O$ was injected into the flask under nitrogen atmosphere. After stirring for 1.5 h at 40 ℃, 20 mL ammonium hydroxide was added dropwise into the solution under vigorous stirring. Finally, the temperature was heated up to 60 ℃ and stirred for 30 min. The products were magnetically collected and washed consecutively with doubly distilled water to neutral. Fe_3O_4-chitosan magnetic nanoparticles were dispersed in 50 mL doubly distilled water.

2.4 Synthesis of CdSeS quantum dots

CdSeS QDs were prepared according to a reported method with some modification.[16] Firstly, the pH of 50 mL precursor solution containing 0.62 mL $CdCl_2$ (0.1 mol L^{-1}) and 1.57 mL (0.1 mol L^{-1}) MPA was adjusted to 9.0 with 1.0 mol L^{-1} NaOH solution. Then, 0.02 mL (0.1 mol L^{-1}) Na_2SeO_3 was added into the precursor solution. Then, the mixed solution was transferred into autoclave, and the temperature was raised to 170 ℃ and remained for 35 min. After cooling down to room temperature, the mixture was purified by addition of 2.5 times the volume of isopropanol and then centrifugation at 10,000 rpm for 5 min. The colloidal precipitate was redissolved in water and freeze-dried for 12 h.

2.5 Synthesis of magnetic and fluorescent CS-Fe_3O_4@CdSeS nanoparticles (MF-CSNPs)

Appropriate amount of Fe_3O_4-chitosan magnetic nanoparticles (pH 4.0) and CdSeS quantum dots (pH 6.5) solutions were added into 0.25 g L^{-1} chitosan solution (pH 4.5) at the same time under stirring. After 1 h, 1.0 mol L^{-1} NaOH solution was added dropwise into chitosan solution until the clear solution turned cloudy. The prepared MF-CSNPs were magnetically separated and washed with doubly distilled water, and then redispersed in doubly distilled water to obtain stock solution. The mass of MF-CSNPs in 1 L stock solution was 1.63 g. The concentration of MF-CSNPs in stock solution was 1.35 mmol L^{-1} represented by the concentration of Cd according to the results of elementary analysis. The stock solution was used directly in the process of removal and detection of copper ion.

2.6 Removal of copper ion

The copper ions in water could be adsorbed on prepared MF-CSNPs and removed with an external magnetic field. Adsorption of copper ion on MF-CSNPs was studied by batch experiments. The adsorption and removal procedures of copper ion were carried out as following: Typically, 5 mL adsorption volume of solution containing 1.0 mL of MF-CSNPs stock solution, 1.0 mL of 0.01 mol L^{-1} phosphate buffer solution (PBS, pH=7.0), and different amount of copper ion was used in each adsorption. All samples were shaken for 30 min, then, the MF-CSNPs were separated using an adscititious

magnet. The remaining concentration of copper ion in the supernatant solution was quantified with flame atomic adsorption spectrometry. The adsorption capacity of MF-CSNPs (Q, mg g^{-1}) was calculated using equation (1):

$$Q = \frac{(C_0 - C) \times V}{m} \quad (1)$$

The removal of copper ion (η) was calculated via equation (2):

$$\eta\% = \frac{(C_0 - C)100}{C_0} \quad (2)$$

Where C_0 and C were the initial and final concentrations of copper ion in aqueous solution (mg L^{-1}), V was the volume of suspension (L), m was the weight of MF-CSNPs (g).

2.7 Analytical procedure for copper ion

The fluorescence quenching of MF-CSNPs was induced by the adsorption of copper ion. The linear relationship between the relative fluorescence intensity of the MF-CSNPs and the concentration of copper ion was investigated. The general procedures for determination of copper ion were carried out as following: In a dry 10 mL colorimeter flask, solutions were added according to the following order: 2.0 mL of 0.01 mol L^{-1} phosphate buffer solution (pH=7.0), a certain volume of MF-CSNPs stock solution, and different amount of copper ion. Then, the solutions were diluted to the mark with doubly distilled water and mixed thoroughly. The relative fluorescence intensity at emission peak 515 nm was measured at room temperature with excitation wavelength 320 nm.

2.8 Detection of copper ion in real water sample

To study the possibility of practical applications in real water samples, addition recovery experiment of copper ion was measured in spring water (Nongfu spring Hubei Dan Jiang Kou Co., Ltd, China) and tap-water sample. In a dry 10 mL colorimeter tube, 2.0 mL 0.01 mol L^{-1} phosphate buffer solution (pH=7.0), 1.0 mL of MF-CSNPs stock solution, 3.0 mL of the city tap-water (or 6.0 mL of the spring water) and different amount of copper ion were added and diluted to the mark with doubly distilled water. The relative fluorescence intensity at emission peak 515 nm was measured at room temperature with excitation wavelength 320 nm.

3. Results and discussion

Novel CS-Fe_3O_4@CdSeS nanoparticles with both magnetic and fluorescent properties were prepared by incorporating Fe_3O_4-chitosan nanoparticles and mercaptopropionic acid capped alloyed CdSeS quantum dots into a chitosan matrix. The structure and properties of these novel MF-CSNPs were investigated. Study on MF-CSNPs for simultaneous removal and determination of copper ion was carried out.

3.1 Characterization of magnetic and fluorescent CS-Fe_3O_4@CdSeS nanoparticles

Fig. 1 shows the ultraviolent-visible and fluorescent emission spectrum of CdSeS quantum dots and CS-Fe_3O_4@CdSeS. It displays that the adsorption and fluorescent emission spectrum of CdSeS quantum dots and MF-CSNPs are almost similar, an absorption peak near 320 nm in UV-Vis spectra and an emission peak at 515 nm in fluorescent emission spectra. The CdSeS quantum dots and MF-CSNPs reveal a symmetric band edge emission with narrow FWHM (the full width at half maximum), thus demonstrating well monodispersity and crystallinity. The combination of Fe_3O_4-chitosan and CdSeS did not significantly vary the energy gap of CdSeS.

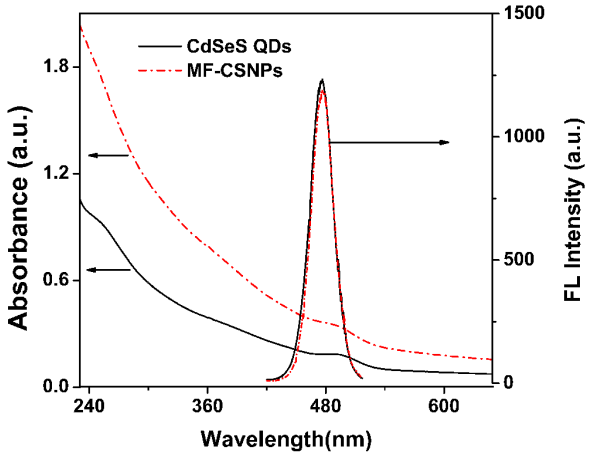

Fig. 1. The ultraviolent-visible spectra and fluorescence spectra of CdSeS QDs and MF-CSNPs with identical concentration of Cd in PBS solution (pH=7.0).

The XRD patterns of the as-prepared Fe_3O_4-chitosan magnetic nanoparticles, CdSeS QDs and MF-CSNPs are showed in Fig. 2. Peaks at 2θ= 30.1, 35.4, 43.0, 56.9, 62.6 can be attributed to crystal planes (220), (311), (400), (511), (440), which were in agreement with the standard XRD JCPDS card of face-centered cubic Fe_3O_4 phase (NO. 65-3107). The diffraction pattern of CdSeS QDs with broad peaks was close to that of CdS nanopartical, implying that crystal structure of CdSeS QDs was similar to that of bulk cubic CdS. As shown in Table 1, the mole ratio of Cd:Se:S in CdSeS QDs was 8:1:8. The elemental composition of the prepared products proved that the prepared CdSeS QDs were mainly CdS capped by mercaptopropionic acid. The conclusion was similar to that reported by Zhan group[16] and Qian group,[29] indicating that alloyed CdSeS QDs with a CdSe-rich core and a CdS-thick shell were synthesized. The XRD pattern of MF-CSNPs matched well with those of Fe_3O_4-chitosan magnetic nanoparticles and CdSeS QDs. As listed in Table 1, the mole ratio of Fe:Cd:Se:S in MF-CSNPs was 3:8:1:6. The results suggested the formation of CS-Fe_3O_4@CdSeS nanoparticles. The mole ratio of Cd:Se:S in MF-CSNPs differed from that in CdSeS QDs, indicating that the assembly of CdSeS QDs and Fe_3O_4-chitoan nanoparticles may induce the loss of CdS or mercaptopropionic acid on the surface of the alloyed CdSeS QDs.

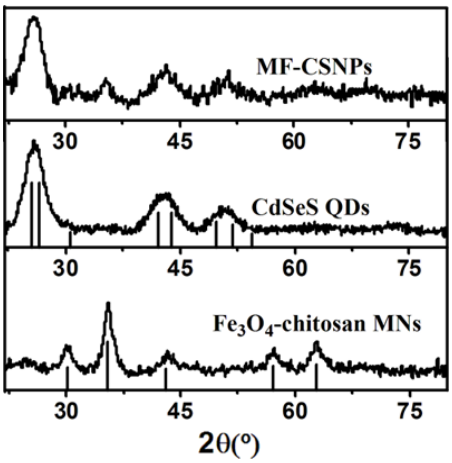

Fig. 2. XRD pattern of Fe_3O_4-chitosan magnetic nanoparticles, CdSeS QDs and MF-CSNPs.

Table 1 The mole ratio of Cd, S, Se and Fe element in CdSeS QDs and MF-CSNPs

	Fe	Cd	S	Se
CdSeS QDs	-	8.93	8.29	1
MF-CSNPs	3.03	8.18	6.36	1

Magnetization of Fe_3O_4-chitosan magnetic nanoparticles and MF-CSNPs were characterized by VSM. Fig. 3 shows the typical M-H plots of the magnetization M (emu g^{-1}) versus the applied magnetic field H (Oe) for Fe_3O_4-chitosan magnetic nanoparticles and MF-CSNPs at room temperature (300K). For both of them, no magnetic hysteresis loops and no remanence were observed from the field-dependent magnetization plots, which illustrated that they were superparamagnetic. The saturation magnetizations (M_S) values of Fe_3O_4-chitosan magnetic nanoparticles and MF-CSNPs were 50.1 emu g^{-1} and 1.5 emu g^{-1}, respectively. M_S is related to the weight of magnetic content in the composite material.[30] The decrease in M_S value of MF-CSNPs as compared with Fe_3O_4-chitosan magnetic nanoparticles was due to the contribution of nonmagnetic chitosan and CdSeS QDs. The MF-CSNPs were well dispersed in doubly distilled water before magnetic separation and could be attracted to the side near the magnetic with clear solution left in minutes. Under 365 nm UV light, MF-CSNPs emitted green fluorescence light (Fig. 3a), which could be observed only at the corresponding site near the magnetic when external magnetic field was applied (Fig. 3b). These results proved that the MF-CSNPs exhibited well magnetic responsibility. The prepared MF-CSNPs showed excellent fluorescence and superparamagnetic properties.

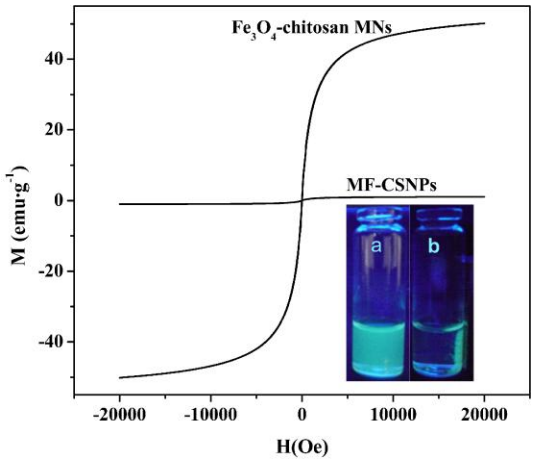

Fig. 3. Magnetization curves of Fe_3O_4-chitosan magnetic nanoparticles and MF-CSNPs. The inset was the color images of MF-CSNPs without (a**)** and with (b**)** magnet capture under 365 nm UV lamp.

The size and morphology of nanocrystal were characterized by TEM. Fig. 4 gives the TEM images of CdSeS QDs, Fe_3O_4-chitosan and MF-CSNPs. The CdSeS QDs have almost spherical shape with the average diameter of 2 nm (Fig 4a). The Fe_3O_4-chitosan magnetic nanoparticles are also almost spherical in shape and with the average diameter of 8 nm (Fig. 4b). MF-CSNPs have similar shape with Fe_3O_4-chitosan magnetic nanoparticles, but they tend to aggregate which may enlarge the particle size (Fig 4c).

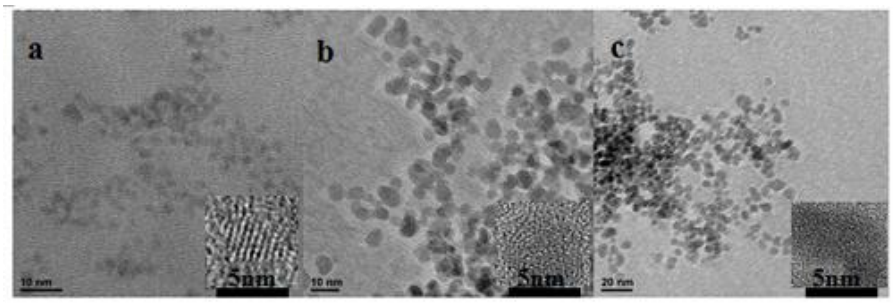

Fig. 4. TEM images of CdSeS QDs (a), Fe_3O_4-chitosan magnetic nanoparticles (b) and MF-CSNPs (c).

Zeta potentials of the samples are shown in Fig. 5. The CdSeS quantum dots bear negative surface charge as pH rangs from 3.0 to 13.0. In the case of MF-CSNPs and Fe_3O_4-chitosan magnetic nanoparticles, a very distinct positive shift of the zeta potential curve was observed. This behaviour can be attributed to the modification of chitosan.

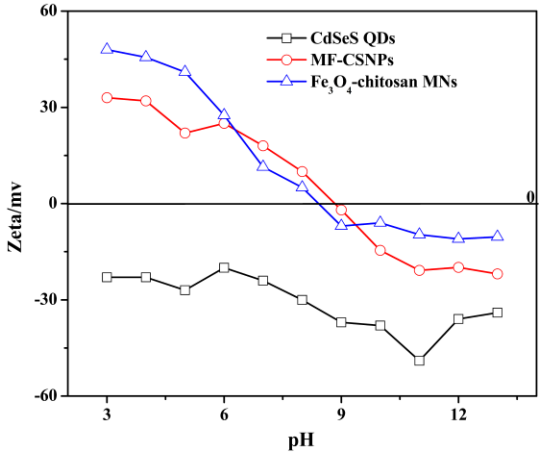

Fig. 5. Zeta potential of CdSeS QDs, Fe_3O_4-chitosan magnetic nanoparticles, and MF-CSNPs.

3.2 Adsorption and removal of copper ion

Adsorption and removal of copper ion from aqueous solution with MF-CSNPs was investigated. In pH 7.0 phosphate buffer solution, the saturated adsorption capacity of MF-CSNPs against copper ion was 260 mg g^{-1} (Fig. 6). As shown in Table 2, the saturated adsorption amount of MF-CSNPs for copper ion was superior to the reported materials.[23,31-33] With MF-CSNPs adsorbent dosage 0.33 g L^{-1}, the removal of copper ion was above 95.0% at concentration below 20 mg L^{-1}. Thus, we can confirm that the obtained MF-CSNPs nanoparticles were admirable adsorbents for copper ion.

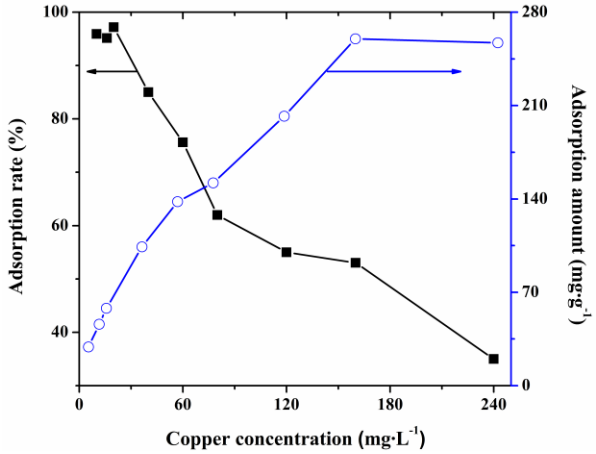

Fig. 6. Adsorption rate (%) and adsorption capacity (mg g^{-1}) of MF-CSNPs for copper ion.

Table 2 The maximum adsorption capacity of reported absorbents for copper ion

Material	Adsorption capacity (mg g^{-1})	Refs
Silanol-functionalized silica	62	31
Mercapto-functionalized silica	51	32
Collagen-tannin resin	16.5	33
Glutathione-modified Fe_3O_4@ZnS	91	23
MF-CSNPs	260	This work

3.3 Detection of copper ion

Copper ions adsorbed on MF-CSNPs could induce the fluorescence quenching of MF-CSNPs, the fluorescence quenching of MF-CSNPs was then investigated for detection of copper ion.

The hydrolysis of copper ion will occur when the pH of solution is beyond 7.5. In acid condition, the fluorescence intensity of MF-CSNPs decreased as a result of the deconstruction of MF-CSNPs due to the protonation of quantum dots.[34] Therefore, PBS of pH 7.0 was selected as buffer solution.

Fig. 7 shows the fluorescence response of MF-CSNPs in the presence of 20 μg Ł$^{-1}$ copper ion as a function of time. It could be seen that the addition of copper ion led to the significant fluorescence quenching of MF-CSNPs, which reached equilibrium in 30 min. The fluorescence signals were stable for more than 90 min. Therefore, the fluorescence intensity was recorded after the system was kept for 30 min.

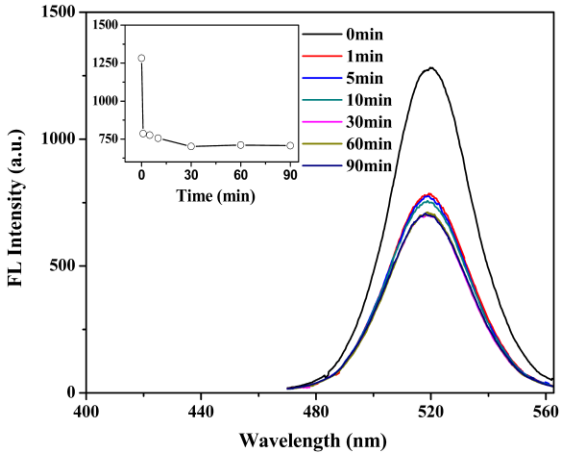

Fig. 7. The fluorescence spectra of MF-CSNPs in the presence of 20 μg Ł$^{-1}$ copper ion measured at different times. The inset showed fluorescence intensity at 515 nm for MF-CSNPs in the presence of 20 μg Ł$^{-1}$ copper ion as a function of measuring time. The excitation wavelength was 320 nm.

Generally, there is a linear relationship between the fluorescence intensity and the concentration of MF-CSNPs. The experimental results showed that the fluorescence intensity increased with the increase of concentration of MF-CSNPs, and reached maximum when MF-CSNPs was 0.47 mmol Ł$^{-1}$ (Fig. 8). It was speculated that relatively higher MF-CSNPs concentration would not generate higher fluorescence intensity because of the inner filter effects and fluorescent self-adsorption.[35] As shown in Fig. 9, the relationship between the fluorescence quenching of MF-CSNPs and copper ion concentration could be described by the conventional linear Stern-Volmer equation (3):

$$\frac{F_0}{F} = C + K_{SV} Q \qquad (3)$$

where F_0 and F are the fluorescence intensities of the samples in the absence and presence of copper ions, respectively. Q is the copper ion concentration (μg Ł$^{-1}$), C is the constant of the equation and K_{SV} is the Stern-Volmer quenching constant. The linear range and limit of detection (LOD) for copper ion is dependent on the concentration of MF-CSNPs. With 0.047 mmol Ł$^{-1}$, 0.14 mmol Ł$^{-1}$ and 0.47 mmol Ł$^{-1}$ MF-CSNPs aqueous solutions, the linear range varied in the copper ion

concentration range 0.21-80 μg Ł$^{-1}$, 0.33-200 μg Ł$^{-1}$, 0.40-700 μg Ł$^{-1}$. The values of K_{SV} were found to be 0.346, 0.129 and 0.0869 with the correlation coefficients of 0.9969, 0.9993, and 0.9949, while the calculated limits of detection were 0.063 μg L^{-1}, 0.10 μg Ł$^{-1}$, and 0.12 μg Ł$^{-1}$, respectively. When relatively high MF-CSNPs concentration was applied, fluorescence quenching caused by the binding reaction between MF-CSNPs and copper ion in the solution was only a little. The extent of the changes in fluorescence intensity was limited with the increasing concentration of copper ions. Relatively larger amount of copper ion could react with MF-CSNPs, thus, there are broad linear range as well as low sensitivity for copper ion. However, low MF-CSNPs concentration means low adsorption amount of copper ion and significant change in the fluorescence intensity of system as the copper ion concentration increasing, it may result in narrow linear range and high sensitivity for detection of copper ion.

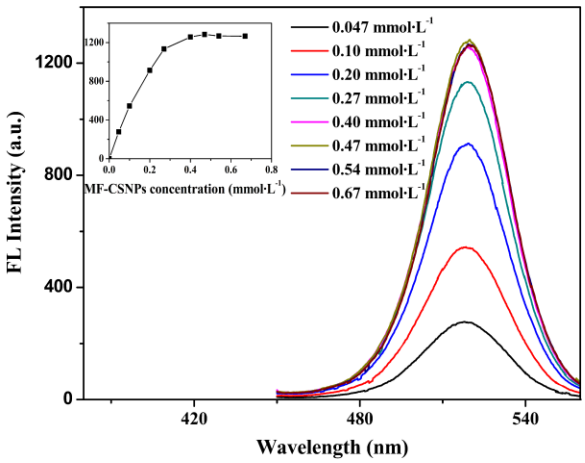

Fig. 8. The fluorescence spectra of different concentration of MF-CSNPs. The inset was the curve of the fluorescence intensity of MF-CSNPs at 515 nm versus the concentration of MF-CSNPs in the 0.047 to 0.67 mmol Ł$^{-1}$ concentration range. The excitation wavelength for the FL spectrum was at 320 nm.

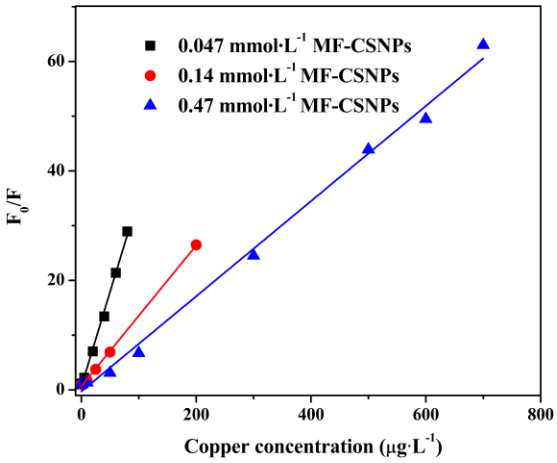

Fig. 9. Calibration curves of the relative fluorescence intensity (F_0/F) of 0.047 mmol Ł$^{-1}$, 0.14 mmol Ł$^{-1}$ and 0.47 mmol Ł$^{-1}$ MF-CSNPs at 515 nm versus different concentration of copper ion. The excitation wavelength was 320 nm.

The relative standard deviation for six replicate measurements was 0.86% with 0.14 mmol Ł$^{-1}$ of MF-CSNPs aqueous solution and 20 μg Ł$^{-1}$ copper ion, indicating satisfactory precision of this method.

Copper ion was enriched and removed from 100 mL solution with MF-CSNPs as adsorbent by applying an adscititious magnet, and then redispersed in 10 mL PBS buffer solution (pH=7.0). The relationship between the fluorescence signals of system after enrichment and copper ion concentration in original solution before enrichment was also investigated. With 0.047 mmol L^{-1} MF-CSNPs aqueous solution, the values of K_{SV} and LOD were found to be 0.598 and 0.022 μg L^{-1}, with the correlation coefficients of 0.9913 (Fig. 10). The enrichment procedure increased the sensitivity and decreased detection limit for determination of copper ion. Compared with reported methods, we find that our method exhibited lower detection limit (Table 3).

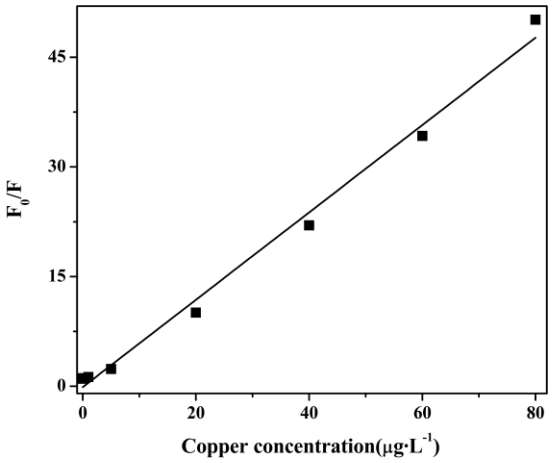

Fig. 10. The calibration curve of the relative fluorescence intensity (F_0/F) of MF-CSNPs (0.047 mmol L^{-1}) at 515 nm after enrichment versus the concentration of copper ion in the original solution before enrichment.

Table 3 Analytical parameters for copper ion compared with other luminescent methods

Reagent	Linear range (μg L^{-1})	LODs (μg L^{-1})	Refs
2,3-modified Bodipy derivatives	0- 256	33.9	36
Glutathione-modified Fe_3O_4-ZnS	320- 1920	12.8	23
MAO-mPEG-CdSe/CdS	0.64-32	1.02	37
MPA-CdSe	0.48-800	0.13	10
Chitosan-CdS	0.512-192	0.0768	38
Chitosan-Fe_3O_4-CdSe	0.125-25	0.046	27
Chitosan-Fe_3O_4-CdSeS	0.073-80 (0.047 mmol L^{-1} MF-CSNPs, enrichment)	0.022	This work

High selectivity is a matter of necessity for an excellent sensor. Therefore, we investigated the interference of potential co-existent ion on the determination of copper ion under the same condition. The experiments were also conducted in 0.14 mmol L^{-1} of MF-CSNPs phosphate buffer solution (PBS, pH=7.0) with copper ion (0.1 mg L^{-1}) and other metal ions (K^+, Na^+, Mg^{2+}, Ca^{2+}, Pb^{2+}, Ni^+, Zn^{2+}, Ba^{2+}, Fe^{3+} and Hg^{2+}, 0.1 mg L^{-1}). The results indicated that the potential co-existent ion

basically would not generate effect on the quenching of fluorescence of MF-CSNPs at given concentration. The obtained MF-CSNPs possess highly selectivity for copper ion over other metal ions (Fig. 11).

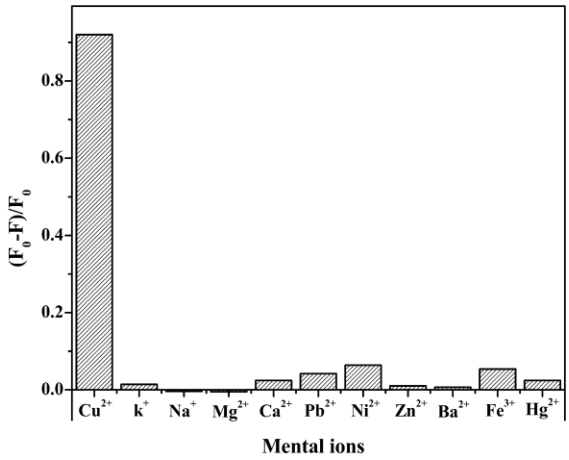

Fig. 11. Bar graph represents the fluorescence-intensity ratios $(F_0 - F)/F_0$ of MF-CSNPs in the presence of different metal ions with the identical concentration.

To investigate the application of MF-CSNPs in analysis of real water sample, the addition recovery experiment was carried out in tap water and spring water, the results of analysis were listed in Table 4. For each sample, three parallel experiments were conducted, and the relative standard deviation (RSD) was 0.63-0.99%. The recovery rates of copper ion for tap water and spring water were found to be 97.1%-106% and 101%-108%, respectively. The calculated concentrations of copper ion in tap water and spring water were 2.73 μg L^{-1} and 0.60 μg L^{-1}, respectively, close to the values obtained with graphite furnace atomic adsorption spectrometry (GFAAS) (data was supplied by Analytical and Testing Center of Wuhan University). The results indicated that the presented method showed good sensitivity and accuracy for determination of copper ion in real water samples. Therefore, the MF-CSNPs were applicable for the ultrasensitive determination of copper ion in real water.

Table 4 Analytical results of real water sample and recovery (n=3)

sample		Content of copper ion			Recovery	RSD
		Added (μg L^{-1})	GFAAS* (μg L^{-1})	This method (μg L^{-1})	(%)	(%)
Tap	1	0	3.03	2.73	-	0.99
water	2	1.67		4.5	106	0.68
	3	3.33		5.97	97.1	0.84
Spring	1	0	No	0.60	-	0.63
water	2	0.83		1.5	108	0.75
	3	1.67		2.28	101	0.67

*:GFAAS data was supplied by Analytical and Testing Center of Wuhan University.

4. Conclusion

In summary, novel bifunctional CS-Fe_3O_4@CdSeS nanoparticles with magnetic and fluorescent properties were successfully synthesized. The obtained CS-Fe_3O_4@CdSeS exhibited good sensitivity and selectivity for simultaneous removal and optical determination of trace copper ions over other metal ions in aqueous solution. The detection limit for copper ions in this method was 0.022 μg L^{-1}, superior to the result of reported method. In particular, the CS-Fe_3O_4@CdSeS possessed excellent adsorption ability for copper ion with the high saturation adsorption capacity of 260 mg g^{-1}, which facilitated efficient removal of copper ion. The above results confirm that novel bifunctional CS-Fe_3O_4@CdSeS nanoparticles are sensitive, selective and low-cost materials for the simultaneous removal and optical detection of copper ion in aqueous solution.

Acknowledgement

Special thanks to the Analytical and Testing Center of Wuhan University for XRD measurement and analysis of water samples, and the School of Physics and Technology in Wuhan University for HRTEM measurement.

Notes and References

1 R. Uauy, M. Olivares and M. Gonzalez, *Am. J. Clin. Nutr.*, 1998, **67**, 952-959.

2 E. Gaggelli, K. Kozlowski, D. Valensin and G. Valensin, *Chem. Rev.*, 2006, **106**, 1995-2044.

3 W. Yantasee, Y. H. Lin, G. E. Fryxell, K. L. Alford, B. J. Busche and C. D. Johnson, *Ind. Eng. Chem. Res.*, 2004, **43**, 2759-2764.

4 M. F. Frasco, and N. Chaniotakis, *Sensors*, 2009, **9**, 7266-7286.

5 P. Wu, T. Zhao, S. L. Wang and X. D. Hou, *Nanoscale*, 2014, **6**, 43-64.

6 Y. B. Lou, Y. X. Zhao, J. X. Chen and J. J. Zhu, *J. Mater. Chem. C.*, 2014, **2**, 595-614.

7 H. Han, G. D. Francesco and M. M. Maye, *J. Phys. Chem. C*., 2010, **114**, 19270-19277.

8 S. Mohan, O. S. Oluwafemi, S. P. Songca, O. A. Osibote, S. C. George, N. Kalarikkal and S. Thomas, *New. J. Chem*., 2014, **38**, 155-162.

9 S. V. Kahane, V. Sudarsan and S. Mahamuni, *J. Lumin*., 2014, **147**, 353-357.

10 K. Zhang, J. K. Guo, J. J. Nie, B. Y. Du and D. J. Xu, *Sensor. Actuat. B.*, 2014, **190**, 279-287.

11 Z. S. Qian, J. J. Ma, X. Y. Shan, L. X. Shao, J. Zhou, J. R. Chen, and H. Feng, *RSC. Adv.*, 2013, **3**, 14571-14579.

12 B. B. Lin, X. Z. Yao, Y. H. Zhu, J. H. Shen, X. L. Yang, H. L. Jiang and X. Q. Zhang, *New. J. Chem.*, 2013, **37**, 3076-3083.

13 L. J. Zhang, X. C. Shen, H. Liang, F. Y. Chen and H. J. Huang, *New. J. Chem*., 2014, **38**, 448-454.

14 F. Li, C. J. Liu, J. Yang, Z. Wang, W. G. Liu and F. Tian, *RSC. Adv.*, 2014, **4**, 3201-3205.

15 K. Saikia, P. Deb and E. Kalita, *Phys. Scr.*, 2013, **87**, 065802.

16 H. J. Zhan, P. J. Zhou, L. Ding, Z. Y. He and R. Ma, *J. Lumin*., 2012, **132**, 2769-2774.

17 A. P. Lim and A. Z. Aris, *Rev. Environ. Sci. Bio.*, 2014, **13**, 163-181.

18 S. Zhou, Q. W. Chen, X. Y. Hu and T. Y. Zhao, *J. Mater. Chem.*, 2012, **22**, 8263-8270.

19 X. Q. Gong, Q. Zhang, Y. Cui, S. J. Zhu, W. Y. Su, Q. Y. Yang and J. Chang, *J. Mater. Chem. B.*, 2013, **1**, 2098-2106.

20 L. Sun, Y. X. Li, M. D. Sun, H. G. Wang, S. F. Xu, C. Q. Zhang and Q. B. Yang, *New. J. Chem*., 2011, **35**, 2697-2704.

21 G. N. Wang, L. Jin, Y. K. Dong, L. Niu, Y. X. Liu, F. Ren and X. G. Su, *New. J. Chem*., 2014, **38**, 700-708.

22 H. G. Wang, L. Sun, Y. P. Li, M. D. Sun, C. Q. Zhang, Y. X. Li and Q. B. Yang, *Langmuir*, 2011, **27**, 11609-11615.

23 P. L. Yang, B. C. Zhu, J. Zhao, H. Q. Yu, L. G. Yan, Q. Wei and B. Du, *Inorg. Chim. Acta*., 2013, **408**, 120-125.

24 M. N.V. Ravi Kumar, *React. Funct. Polym.*, 2000, **46**, 1-27.

25 M. Rinaudo, *Prog. Polym. Sci.*, 2006, **31**, 603-632.

26 D. H. K. Reddy and S-M Lee, *Adv. Colloid. Interfac.*, 2013, **201-202**, 68-93.

27 L. Liu, L. Xiao. H. Y. Zhu and X. W. Shi, *Microchim. Acta*., 2012, **178**, 413-419.

28 W. Li, L. Xiao and C. Q. Qin, *J. Macromol. Sci. A.*, 2011, **48**, 57-64.

29 H. F. Qian, L. Li and J. C. Ren, *Mater. Res. Bull*., 2005, **40**, 1726-1736.

30 S. Braconnot, M. M. Eissa and A. Elaissari, *Colloid. Polym. Sci*., 2013, **291**, 193-203.

31 Y. G. Wang, S. J. Huang, S. F. Kang, C. L. Zhang and X. Li, *Mater. Chem. Phys.*, 2012, **132**, 1053-1059.

32 S. Štandeker, A. Veronovski, Z. Novak and Ž. Knez, *Desalination*, 2011, **269**, 223-230.

33 X. Sun, X. Huang, X. P. Liao and B. Shi, *J. Hazard. Mater.*, 2011, **186**, 1058-1063.

34 M. Y. Gao, S. Kirstein, H. Möhwald, A. L. Rogach, A. Kornowski, A. Eychmüller and H. Weller, *J. Phys. Chem. B*., 1998, **102**, 8360-8363.

35 M. O. Palmier and S. R. Van Doren, *Anal. Biochem.*, 2007, **371**, 43-51.

36 J. B. Wang, Y. J. Xie, Z. Wang and Q. H. Song, *Sensor. Actuat. B*., 2014, **194**, 149-155.

37 Z. Cao, Z. Gu, J. L. Zeng, J. H. Liu, Q. Deng, J. B. Fan, and J. N. Xiang, *Anal. Sci*., 2011, **47**, 643-647.

38 S. J. Lai, X. J. Chang and C. Fu, *Microchim. Acta*., 2009, **165**, 39-44.